Available online at www.sciencedirect.com
SCIENCE DIRECT®
Mathematics and Computers in Simulation 69 (2005) 457–466
MATHEMATICS AND COMPUTERS IN SIMULATION
www.elsevier.com/locate/matcom

Numerical integration of the plasma fluid equations with a modification of the second-order Nessyahu–Tadmor central scheme and soliton modeling

R. Naidoo[a], S. Baboolal[b,*]

[a] *Department of Mathematics, Durban Institute of Technology, Steve Biko Campus, P.O. Box 953, Durban 4000, South Africa*
[b] *School of Computer Science, University of KwaZulu-Natal, Westville Campus, Private Bag X54001, Durban 4000, South Africa*

Available online 1 June 2005

Abstract

Here we outline a modification of the second order central difference scheme based on staggered spatial grids due to Nessyahu and Tadmor [H. Nessyahu, E. Tadmor, Non-oscillatory central differencing for hyperbolic conservation laws, J. Comput. Phys. 87 (1990) 408] to a non-staggered scheme for one-dimensional hyperbolic systems which can additionally include source terms. With this modification we integrate the one-dimensional electrostatic plasma fluid-Poisson equations to illustrate ion-acoustic soliton formation and propagation. This application is interesting because, to our knowledge, it is the first time that a high-resolution scheme has been employed on the plasma fluid equations, where in particular, we test its ability to handle a coupled fluid-Poisson system and also, we examine its performance on very long time integrations involving thousands of time steps. As a check on the accuracy of the modified scheme we perform tests on a shock capturing problem in a Broadwell gas, and in both cases, the results obtained are compared with those from previously reported schemes.
© 2005 IMACS. Published by Elsevier B.V. All rights reserved.

Keywords: Non-staggered scheme; Hyperbolic systems; Shock capturing; Plasma solitons

* Corresponding author.
E-mail addresses: naidoor@dit.ac.za (R. Naidoo); baboolals@ukzn.ac.za (S. Baboolal).

0378-4754/$30.00 © 2005 IMACS. Published by Elsevier B.V. All rights reserved.
doi:10.1016/j.matcom.2005.03.010

1. Introduction

Hyperbolic systems of partial differential equations can be used to model many physical systems, including fluids and electrical plasmas. The Riemann-solver-free high-resolution staggered second-order scheme of Nessyahu and Tadmor [1] has been a prototype for several that were devised for the numerical solution of hyperbolic systems. Most of these were obtained for or applied to homogeneous systems. Moreover, the use of staggered schemes complicates the application of boundary conditions. Jiang et al. [2] formulated a procedure to convert staggered schemes to non-staggered ones for systems without source terms. In this paper we combine the above methods [1,2] to produce a non-staggered second-order numerical scheme to integrate hyperbolic systems which include source terms. This is an alternative to the use of splitting methods for source terms [3,4]. We test it by modeling shocks in a Broadwell gas [3,4]. We then model ion-acoustic soliton formation and evolution in an electrical plasma fluid composed of ideal-gas electron and ion fluids [5].

The modified technique outlined here is applicable to the numerical integration of a one-dimensional system in the general form:

$$\frac{\partial u(x,t)}{\partial t} + \frac{\partial f(u)}{\partial x} = g(u). \tag{1}$$

Here $u(x,t)$ is the unknown m-dimensional vector function, $f(u)$ the flux vector, $g(u)$ a continuous source vector function, with x the single spatial coordinate and t the temporal coordinate.

In Section 2 we outline the modifications required in the numerical scheme [1] and Section 3 reports on a test application for a Broadwell gas and then on its application to ion-acoustic solitons in a two-fluid plasma.

2. The modified numerical scheme

Although this treatment follows closely those of [1,2] and a later elucidation in [6], we shall find it instructive to follow first principles in order to clarify the incorporation of the source term, but we nevertheless omit many details. To begin, we employ uniform spatial and temporal grids with the spacings, $\Delta x = x_{j+1} - x_j$; $\Delta t = t^{n+1} - t^n$ (j and n being suitable integer indices).

Now we apply the concept of a weak solution [7,8], and integrate (1) over the cell $[x_j, x_{j+1}] \times [t^n, t^{n+1}]$ as

$$\int\int \frac{\partial u}{\partial t}\,\mathrm{d}t\,\mathrm{d}x + \int\int \frac{\partial f}{\partial x}\,\mathrm{d}t\,\mathrm{d}x = \int\int g(u)\,\mathrm{d}t\,\mathrm{d}x. \tag{2}$$

Then, with the definition:

$$\frac{1}{\Delta x}\int u(x,t^{n+1})\,\mathrm{d}x = \overline{u}^{n+1}_{j+(1/2)}, \tag{3}$$

which are cell averages centred at $x_{j+(1/2)}$ with support $[x_j, x_{j+1}]$ we follow [1] and obtain from (2)

$$\overline{u}^{n+1}_{j+(1/2)} = \frac{1}{\Delta x}\int_{x_j}^{x_{j+1}} u(x,t^n)\,\mathrm{d}x - \frac{1}{\Delta x}\int_{t^n}^{t^{n+1}}\int_{x_j}^{x_{j+1}} \frac{\partial f}{\partial x}\,\mathrm{d}x\,\mathrm{d}t + \frac{1}{\Delta x}\int_{t^n}^{t^{n+1}}\int_{x_j}^{x_{j+1}} g(u)\,\mathrm{d}x\,\mathrm{d}t \tag{4}$$

To proceed, we employ for $u(x, t^n)$ in the integral above, piece-wise linear approximations of the form:

$$L_j^n(x) = \overline{u}_j^n + \frac{x - x_j}{\Delta x} u_{xj}^n, \quad x_{j-(1/2)} \le x < x_{j+(1/2)}, \tag{5}$$

which are the high resolution "MUSCL" type interpolants of [2] where $\overline{u}_j^n$ is the cell average centred at x_j, similar to (3), and the $u_{xj}^n/\Delta x$ denote the discrete slopes, to be explicitly determined later.

Now using (5) for each half interval and following [2], the first integral in (4) is

$$\begin{aligned}\frac{1}{\Delta x}\int_{x_j}^{x_{j+1}} u\,(x, t^n)\,\mathrm{d}x &= \frac{1}{\Delta x}\int_{x_j}^{x_{j+(1/2)}} L_j^n(x)\,\mathrm{d}x + \frac{1}{\Delta x}\int_{x_{j+(1/2)}}^{x_{j+1}} L_{j+1}^n(x)\,\mathrm{d}x \\ &= \frac{1}{2}\overline{u}_j^n + \frac{u_{xj}^n}{8} + \frac{1}{2}\overline{u}_{j+1}^n - \frac{u_{xj+1}^n}{8}\end{aligned} \tag{6}$$

Substituting (6) into (4) then yields

$$\begin{aligned}\overline{u}_{j+(1/2)}^{n+1} = \frac{1}{2}[\overline{u}_j^n + \overline{u}_{j+1}^n] + \frac{1}{8}[u_{xj}^n - u_{xj+1}^n] - \frac{1}{\Delta x}\int_{t^n}^{t^{n+1}}\int_{x_j}^{x_{j+1}} \frac{\partial f}{\partial x}\,\mathrm{d}x\,\mathrm{d}t \\ + \frac{1}{\Delta x}\int_{t^n}^{t^{n+1}}\int_{x_j}^{x_{j+1}} g(u)\,\mathrm{d}x\,\mathrm{d}t.\end{aligned} \tag{7}$$

The flux and source term integrals are now approximated by using the trapezoidal rule in contrast to the use of the midpoint rule for the flux integral in [1]. We have found this approach to give more stable computations especially for the numerical integrations of the plasma fluid equations.

Thus

$$\frac{1}{\Delta x}\int_{t^n}^{t^{n+1}} [f(u(x_j, t)) - f(u(x_{j+1}, t))]\,\mathrm{d}t \quad \simeq -\frac{\lambda}{2}[(f_{j+1}^{n+1} + f_{j+1}^n) - (f_j^{n+1} + f_j^n)] \tag{8}$$

and

$$\frac{1}{\Delta x}\int_{t^n}^{t^{n+1}}\int_{x_j}^{x_{j+1}} g(u(x, t))\,\mathrm{d}x\,\mathrm{d}t \quad \simeq \frac{1}{4}\Delta t[g(u_j^n) + g(u_{j+1}^n) + g(u_j^{n+1}) + g(u_{j+1}^{n+1})], \tag{9}$$

where $\lambda = \Delta t/\Delta x$. Substituting (8) and (9) into Eq. (7) then results in

$$\begin{aligned}\overline{u}_{j+(1/2)}^{n+1} = \frac{1}{2}[\overline{u}_j^n + \overline{u}_{j+1}^n] + \frac{1}{8}[u_{xj}^n - u_{xj+1}^n] \quad - \frac{\lambda}{2}[(f_{j+1}^{n+1} + f_{j+1}^n) - (f_j^{n+1} + f_j^n)] \\ + \frac{\Delta t}{4}[g(u_j^n) + g(u_{j+1}^n) + g(u_j^{n+1}) + g(u_{j+1}^{n+1})],\end{aligned} \tag{10}$$

where again the spatial derivative terms are as yet unspecified.

Similarly

$$\begin{aligned}\overline{u}_{j-(1/2)}^{n+1} = \frac{1}{2}[\overline{u}_{j-1}^n + \overline{u}_j^n] + \frac{1}{8}[u_{xj-1}^n - u_{xj}^n] - \frac{\lambda}{2}[(f_j^{n+1} + f_j^n) - (f_{j-1}^{n+1} + f_{j-1}^{n+1})] \\ + \frac{\Delta t}{4}[g(u_{j-1}^n) + g(u_j^n) + g(u_{j-1}^{n+1}) + g(u_j^{n+1})].\end{aligned} \tag{11}$$

We note that (10) is essentially the second-order NT scheme [1] but now includes the source term. Also the $\overline{u}$ terms may be considered [6] to be approximations of the u values at the grid points to second order. Further, since the trapezoidal rule for the flux and source terms integrals are also second-order accurate in space and in time, the overall scheme is second-order accurate.

To obtain the modified form of (10) or (11) for unstaggered grids we proceed as in [2]. First we obtain a piecewise-constant reconstruction from the calculated staggered cell-averages at time t^{n+1} and then project the interpolant onto the nonstaggered grid to obtain non-staggered cell-averages.

Thus, using the definition of the unstaggered cell averages:

$$\overline{u}_j^{n+1} = \frac{1}{\Delta x}\left[\int_{x_{j-(1/2)}}^{x_j} L_{j-(1/2)}^{n+1}(x)\,\mathrm{d}x + \int_{x_{j+(1/2)}}^{x_{j+1}} L_{j+(1/2)}^{n+1}(x)\,\mathrm{d}x\right], \tag{12}$$

employing piecewise-linear interpolants $L_{j\pm(1/2)}^{n+1}$ through the calculated staggered cell-averages at time t^{n+1}, results in

$$\begin{aligned}\overline{u}_j^{n+1} = {} & \frac{1}{\Delta x}\int_{x_{j-(1/2)}}^{x_j} \overline{u}_{j-(1/2)}^{n+1}\,\mathrm{d}x + \frac{1}{\Delta x}\int_{x_j}^{x_{j+(1/2)}} \overline{u}_{j+(1/2)}^{n+1}\,\mathrm{d}x + \frac{u_{xj-(1/2)}^{n+1}}{\Delta x^2}\int_{xj-(1/2)}^{x_j}(x - x_{j-(1/2)})\,\mathrm{d}x \\ & + \frac{u_{xj+(1/2)}^{n+1}}{\Delta x^2}\int_{x_j}^{x_{j+(1/2)}}(x - x_{j+(1/2)})\,\mathrm{d}x \quad = \frac{1}{2}[\overline{u}_{j-(1/2)}^{n+1} + \overline{u}_{j+(1/2)}^{n+1}] - \frac{1}{8}[u_{xj+(1/2)}^{n+1} - u_{xj-(1/2)}^{n+1}],\end{aligned} \tag{13}$$

as in [2].

Substituting Eqs. (10) and (11) into (13) finally gives the second order formula:

$$\begin{aligned}\overline{u}_j^{n+1} = {} & \frac{1}{4}[\overline{u}_{j+1}^{n} + 2\overline{u}_j^{n} + \overline{u}_{j-1}^{n}] - \frac{1}{16}[u_{xj+1}^{n} - u_{xj-1}^{n}] - \frac{1}{8}[u_{xj+(1/2)}^{n+1} - u_{xj-(1/2)}^{n+1}] \\ & + \frac{\Delta t}{8}[g(u_{j+1}^{n}) + 2g(u_j^{n}) + g(u_{j-1}^{n})] + \frac{\Delta t}{8}[g(u_{j+1}^{n+1}) + 2g(u_j^{n+1}) + g(u_{j-1}^{n+1})] \\ & - \frac{\lambda}{4}[(f_{j+1}^{n} - f_{j-1}^{n}) + (f_{j+1}^{n+1} - f_{j-1}^{n+1})].\end{aligned} \tag{14}$$

As is common in shock calculations we shall employ the min-mod derivatives [1–3]:

$$u_{xj-(1/2)}^{n+1} = \mathrm{MM}(\Delta u_j^{n+1}, \Delta u_{j-1}^{n+1}), \quad u_{xj+(1/2)}^{n+1} = \mathrm{MM}(\Delta u_{j+1}^{n+1}, \Delta u_j^{n+1}) \tag{15}$$

where the min-mod nonlinear limiter MM is defined by

$$\mathrm{MM}(s_1, s_2, \ldots) = \begin{cases} \min\{s_j\} & \text{if } s_j > 0\,\forall j \\ \max\{s_j\} & \text{if } s_j < 0\,\forall j \\ 0 & \text{otherwise} \end{cases}$$

and where after some simplification:

$$\begin{aligned}\Delta u_j^{n+1} &= \overline{u}_{j+(1/2)}^{n+1} - \overline{u}_{j-(1/2)}^{n+1} \\ &= \frac{1}{2}[\overline{u}_{j+1}^{n} - \overline{u}_{j-1}^{n}] - \frac{1}{8}[u_{xj+1}^{n} - 2u_{xj}^{n} + u_{xj-1}^{n}] - \frac{\lambda}{2}[f_{j+1}^{n+1} - 2f_j^{n+1} + f_{j-1}^{n+1} \\ &\quad + f_{j+1}^{n} - 2f_j^{n} + f_{j-1}^{n}] + \frac{\Delta t}{4}[g(u_{j+1}^{n+1}) - g(u_{j-1}^{n+1}) + g(u_{j+1}^{n}) - g(u_{j-1}^{n})]. \end{aligned} \tag{16}$$

Here again the u_x terms are evaluated by the min-mod forms:

$$u_{xj} = \mathrm{MM}(u_{j+1} - u_j, u_j - u_{j-1}). \tag{17}$$

Also useful in some applications is the more accurate UNO derivative [1]

$$\begin{aligned} u_{xj} &= \mathrm{MM}(u_j - u_{j-1} + \frac{1}{2}\mathrm{MM}(u_j - 2u_{j-1} + u_{j-2}, u_{j+1} - 2u_j + u_{j-1}), \\ &\quad u_{j+1} - u_j - \frac{1}{2}\mathrm{MM}(u_{j+1} - 2u_j + u_{j-1}, u_{j+2} - 2u_{j+1} + u_j)). \end{aligned} \tag{18}$$

Now, in order to apply the scheme (14), which is implicit in time, we shall require a predictor such as [2]:

$$u^{n+1} = u^n + \Delta t \left[g(u^n) - \frac{1}{\Delta x} f_x^n \right], \tag{19}$$

where the flux spatial derivative terms $\frac{1}{\Delta x} f_x^n$ are at the indicated time level n and can be evaluated using the MM function or calculated from the explicit form of $f(u)$ and (17) or (18).

With these and (15)–(19) we shall hereafter refer to the non-staggered scheme (14) as the NNT scheme.

Some insight can be gained into the stability of the scheme, albeit of the homogeneous form, by performing a von Neumann linear stability analysis [10] of the NNT scheme (14) without the source term. By numerically obtaining the amplification factor as a function of phase angle for various λa, where a is the wave speed obtained by employing Roe's scheme for the Euler equation [10], we have established that the linearized homogeneous version of (14) satisfies the von Neumann necessary condition $|\lambda a| \leq 0.5$ as in [1]. In practice however, for some cases the bound on the right can be taken close to unity.

3. Tests and plasma soliton modeling

3.1. Shocks in a Broadwell gas

First as a test for this scheme we solve the governing equations for a Broadwell gas [3,4]:

$$\frac{\partial \rho}{\partial t} + \frac{\partial m}{\partial x} = 0, \qquad \frac{\partial m}{\partial t} + \frac{\partial z}{\partial x} = 0, \qquad \frac{\partial z}{\partial t} + \frac{\partial m}{\partial x} = \frac{1}{\varepsilon}(\rho^2 + m^2 - 2\rho z),$$

where ε is the mean free path and $\rho(x,t)$, $m(x,t)$, $z(x,t)$ are the density, momentum and flux respectively. The range $\varepsilon = 1 \cdots 10^{-8}$ covers the regime from the non-stiff to the highly stiff. In particular, the limit

$\varepsilon = 10^{-8}$ requires a renormalization of the variables such as in the form:

$$\bar{x} = \frac{1}{\varepsilon}x, \quad \bar{t} = \frac{1}{\varepsilon}t$$

followed by computations on an equivalent finer grid (see for example [9]).

We comment further that in the limit $\varepsilon \to 0$ we obtain

$$z = z_{\mathrm{E}}(\rho, m) = \frac{1}{2\rho}(\rho^2 + m^2)$$

which leads to the equilibrium solution of the governing equations above which they reduce to corresponding Euler equations.

The NNT scheme (14) together with the UNO limiter (18) was applied to the above with the two sets ($Rim1$ and $Rim2$) of initial conditions corresponding to several Riemann problems, each distinguished by a specific ε-value:

$$Rim1 : \rho = 2, m = 1, z = 1, \quad x < x_J, \qquad \rho = 1, m = 0.13962, z = 1, \quad x > x_J.$$

$$Rim2 : \rho = 1, m = 0, z = 1, \quad x < x_J, \qquad \rho = 0.2, m = 0, z = 1, \quad x > x_J.$$

In all calculations absorbing boundary conditions were employed, where in particular, the boundary values were obtained by quadratic extrapolations of internal point values on a fixed grid, over an integration domain D on the X-axis as detailed below. Results obtained are depicted in Fig. 1, as follows:

(a) The rarefied regime ($Rim1$ with $\varepsilon = 1$). The solution shown at time $t = 0.5$ agrees very well with the reference or 'exact' solution obtained by computing with a finer grid with $\Delta x = 0.001$ and $\Delta t = 0.0005$. These results are as good as the staggered grid solutions [3,4].
(b) The intermediate regime ($Rim1$ with $\varepsilon = 0.02$). The solution again agrees very well with the 'exact' solution obtained by computing with the same finer grid as (a) above and with the staggered grid solutions [3,4].
(c) The near fluid dynamic regime ($Rim1$ with $\varepsilon = 10^{-8}$). Here, the computed solution shown agrees reasonably well with the reference and just as well as with the staggered grid solutions [3,4].
(d) The near fluid dynamic regime ($Rim2$ with $\varepsilon = 10^{-8}$). Again here the computed solution agrees reasonably well with the reference and staggered grid solutions [3,4], when one takes into account the fact that the figure gives a "zoomed" view of a subdomain. Also the NNT scheme captures the correct behaviour given in [4]: we observe here a left-moving rarefaction and a right-moving shock wave as in [4].

In general, from (a) and (b) above, we see that the NNT scheme maintains reasonably uniform accuracy when moving from the rarefied regime to the fluid dynamic limit for the Broadwell model; the non-oscillatory properties were confirmed in both the $Rim1$ and $Rim2$ cases with different relaxation times, in agreement with [3,4]. Moreover, the NNT scheme can be applied to systems with source terms that are both stiff and non-stiff, capturing the behaviour predicted by the Broadwell equations as before [3,4].

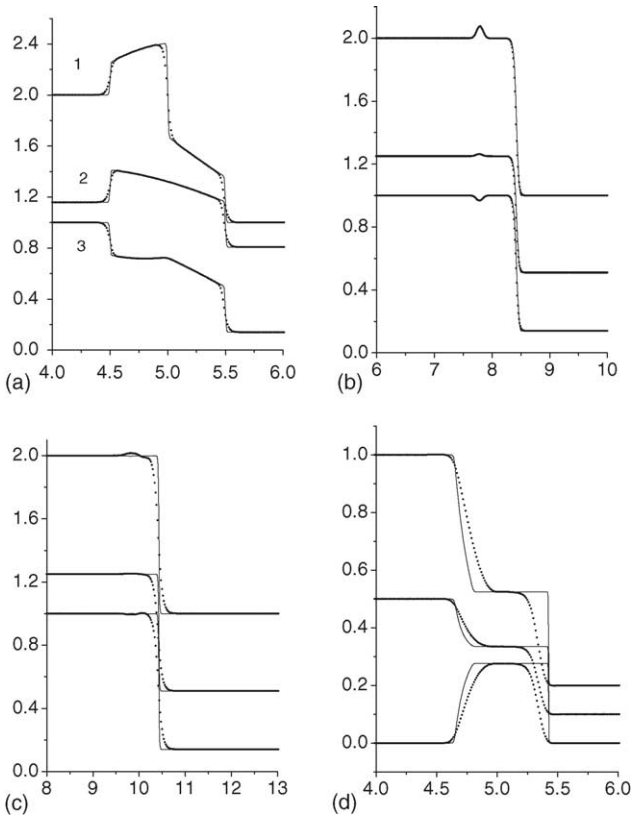

Fig. 1. Broadwell gas shock solutions: (a) *Rim*1 with $\varepsilon = 1$, $D = [0, 10]$, $\Delta x = 0.01$, $\Delta t = 0.005$, $x_J = 5$. (b) *Rim*1 with $\varepsilon = 0.02$, $D = [0, 16]$, $\Delta x = 0.01$, $\Delta t = 0.005$, $x_J = 8$. (c) *Rim*1 with $\varepsilon = 10^{-8}$, $D = [0, 20]$, $\Delta x = 0.02$, $\Delta t = 0.001$, $x_J = 10$. (d) *Rim*2 with $\varepsilon = 10^{-8}$, $D = [0, 10]$, $\Delta x = 0.01$, $\Delta t = 0.005$, $x_J = 5$. Here, the curve labelled $1 \sim \rho$, $2 \sim m$, $3 \sim z$, the snap-shot time is $t = 0.5$ in all cases and the continuous line denotes a reference ("exact") solution.

3.2. Ion-acoustic solitons in a plasma fluid

3.2.1. The electrostatic plasma fluid equations

As our main application, we use the form (1) as a model for an unmagnetized one-dimensional fluid plasma. Here we numerically solve, self-consistently, the one-dimensional Euler–Poisson equations for an unmagnetized plasma consisting of electrons ($k = \mathrm{e}$) and ions ($k = \mathrm{i}$) taken as ideal fluids together with the ideal gas law [5], namely,

Continuity:

$$\frac{\partial n_k}{\partial t} + \frac{\partial (n_k v_k)}{\partial x} = 0. \tag{20}$$

Momentum conservation:

$$m_k n_k \left(\frac{\partial v_k}{\partial t} + v_k \frac{\partial v_k}{\partial x} \right) + \frac{\partial p_k}{\partial x} = -q_k n_k \frac{\partial \phi}{\partial x}. \tag{21}$$

Ideal gas equation of state for each fluid component:

$$p_k n_k^{-\gamma_k} = \text{constant}. \tag{22}$$

Poisson's equation for the electric potential:

$$\frac{\partial^2 \phi}{\partial x^2} = -4\pi \sum_{k=\text{e,i}} q_k n_k. \tag{23}$$

The n_k, v_k, p_k, γ_k, m_k and q_k are the respective component densities, flow velocities, partial pressures, adiabatic indices, particle masses and charges and ϕ is the electric potential. The final equations were suitably normalized to time and spatial scales appropriate for the observation of ion-acoustic wave structures: full details are given in [5]. Also there, it is detailed how the above equations may be written in both conservation and quasilinear forms, where the latter is hyperbolic.

Now for the numerical integration we employ a system length $L_x = 256$, with $\Delta x = 0.1$, an artificial ion/electron mass ratio of 50, an ion/electron temperature ratio of 1/100 together with $\Delta t = 0.01$.

To compute with this scheme we have to employ an implicit procedure. We note that the right-hand side (20)-(21) is not strictly in the form given in (1). However, the fact that ϕ is determined as a function of n_k and v_k by solving the Poisson equation "frozen in time" and then self-consistently incorporating it within the overall algorithm, allows us to treat it as a source term of the type in (1). Full algorithmic details are given in [5], but now with the numerical scheme (14) replacing the older one there.

3.2.2. Soliton computations

In our illustrative application, we demonstrate how solitons can be generated from an initial density perturbations of the form

$$n_k(x, 0) = 1.0 + \exp\left[-\frac{1}{2}(x - x_c)^2\right]; \quad 0 \le x \le L_x \quad (k = \text{e, i})$$

where x_c is the system centre and $L_x = 256$ is its length (see [5] for more details). The initial velocities of the ions and electrons were set to zero for all x. Here, we employ the reflective boundary conditions [5] i.e. the homogeneous Neumann conditions on the densities ($\partial n_k/\partial x = 0$) with zero flow velocities ($v_k = 0$) and zero potentials and electric fields there. The NNT solutions were computed with (14) together with the min-mod limiter (17).

The results given in Fig. 2 illustrate the formation of a double soliton from a density "slug", a device employed in past simulations and experiments (see [5] and references therein). The subsequent evolution, propagation and reflection of the solitons from the boundaries are clearly indicated in for example, the density profiles. Such results have been reported with the use of a more conventional Lax–Wendroff (LW)-type numerical integration scheme [5] and this example is again employed here for comparison purposes. The high-frequency oscillations seen in the electron velocity profiles (curves 3) are predominantly due to the production of electron plasma waves [5] rather than any numerical instabilty. However, at about

Fig. 2. Formation and time evolution of Gaussian density-perturbation induced solitons in a plasma fluid. Here the curve labelled $1 \sim n_e + 0.5$, $2 \sim n_i$, $3 \sim v_e + 0.5$, $4 \sim v_i$, $5 \sim \phi - 1$, where, $n_e(n_i)$ is the electron (ion) number density, $v_e(v_1)$ is the electron (ion) flow velocity, ϕ is the electrostatic potential, all in normalized units. Horizontal distances are in normalized units. Only the starting density profiles $n_i(x) = n_e(x)$ are shown in the initial frames.

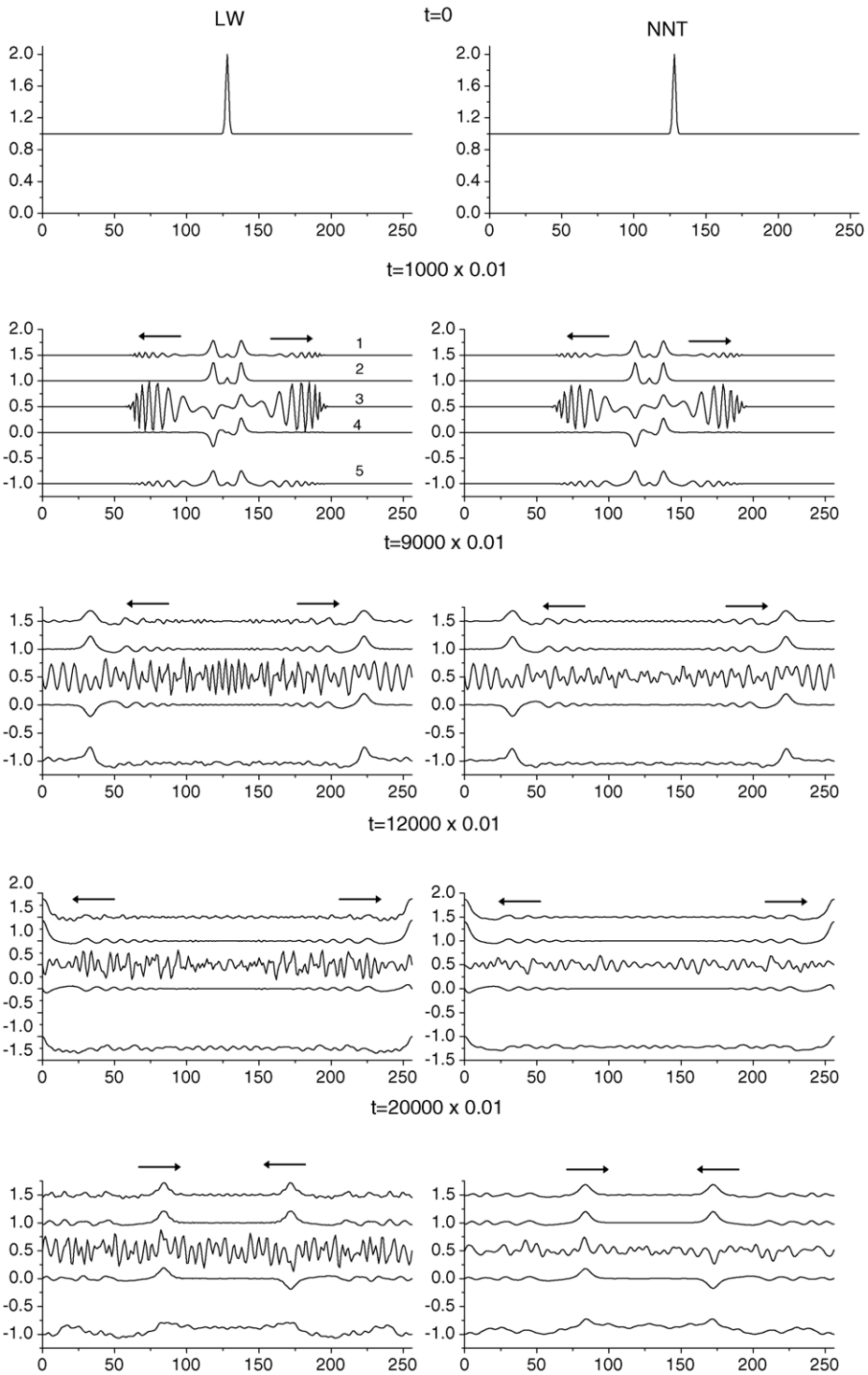
LW
t=0
NNT
t=1000 x 0.01
1
2
3
4
5
t=9000 x 0.01
t=12000 x 0.01
t=20000 x 0.01

this time the soliton structures are reflected at the boundaries. Thereafter, one can observe a significant reduction in the random oscillations in the profiles (e.g. curves 3) of the NNT scheme in comparison to the LW solutions. We suggest that the LW signatures have significant numerical noise over and above any physical waves. Since this noise mainly occurs after the boundary reflections we ascribe it to the inability of the LW scheme to incorporate the imperfect numerical treatment of reflections at the boundaries.

As far as the dissipation of the two schemes is concerned, they appear to be on par, with only a small drop in soliton amplitudes seen in the NNT soliton structures in comparison (see curves 1 and 2 after about 15,000 time steps). This behaviour is due to inherent dissipation [6] of such a scheme and manifests when $\Delta t \sim (\Delta x)^2$ as is the situation here. Nevertheless the NNT scheme is noticeably stable and devoid of spurious oscillations.

4. Conclusion

A version of the Nessyahu–Tadmor [1] scheme for numerical integration of one-dimensional hyperbolic systems with source terms on non-staggered grids has been obtained and employed to integrate the plasma fluid equations. Initial test application of it to model shock structures in a Broadwell gas [3,4] indicate that results are of comparable accuracy to previous staggered scheme results and in some cases of better accuracy to those from Runge–Kutta splitting schemes [3,4]. In our main application of the modeling of the formation of and the long-time evolution of ion-acoustic solitons in a plasma fluid, we find that the scheme is able to contain spurious oscillations due to boundary reflections. We can thus advocate the use of such high-resolution schemes as stable modeling engines in nonlinear plasma studies.

References

[1] H. Nessyahu, E. Tadmor, Non-oscillatory central differencing for hyperbolic conservation laws, J. Comput. Phys. 87 (1990) 408–463.
[2] G.-S. Jiang, D. Levy, C.-T. Lin, S. Osher, E. Tadmor, High-resolution non-oscillatory central schemes with non-staggered grids for hyperbolic conservation laws, SIAM J. Num. Anal. 35 (1998) 2147–2168.
[3] R.E. Caflisch, S. Jin, G. Russo, Uniformly accurate schemes for hyperbolic systems with relaxation, SIAM J. Num. Anal. 34 (1997) 246–281.
[4] S. Jin, Runge-Kutta methods for hyperbolic conservation laws with stiff relaxation terms, J. Comput. Phys. 122 (1995) 51–67.
[5] S. Baboolal, Finite-difference modeling of solitons induced by a density hump in a plasma multi-fluid, Math. Comput. Simul. 55 (2001) 309–316.
[6] A. Kurganov, E. Tadmor, New high-resolution central schemes for nonlinear conservation laws and convection-diffusion equations, J. Comput. Phys. 160 (2000) 241–282.
[7] E.F. Toro, Riemann Solvers and Numerical Methods for Fluid Dynamics, Springer, London, 1999.
[8] R.J. LeVeque, Numerical Methods for Conservation Laws: Lectures in Mathematics, Birkhauser-Verlag, New York, 1992.
[9] G. Naldi, L. Pareschi, Numerical schemes for hyperbolic systems of conservation laws with stiff diffusive relaxation, SIAM J. Num. Anal. 37 (2000) 1246–1270.
[10] C. Hirsch, Numerical Computation of Internal and External Flows, vols. 1 and 2, Wiley, Sussex, 1997.